

Synthesis of 2-pyridone-fused 2,2'-bipyridine derivatives. An unexpectedly complex solid state structure of 3,6-dimethyl-9H-4,5,9-triazaphenanthren-10-one

Stefán Jónsson,^a Carlos Solano Arribas,^a Ola F. Wendt,^b Jay S. Siegel^c and Kenneth Wärnmark^{*a}

^a Organic Chemistry 1, Dept. of Chemistry, Lund University, P.O. Box 124, SE-22100 Lund, Sweden. E-mail: kenneth.warnmark@orgk1.lu.se; Fax: +46 46 2224119; Tel: +46 46 2228217

^b Inorganic Chemistry, Dept. of Chemistry, Lund University, P.O. Box 124, SE-22100 Lund, Sweden

^c Organisch-chemisches Institut, Universität Zürich, Zürich, CH-8057, Switzerland

Received 18th November 2004, Accepted 2nd February 2005

First published as an Advance Article on the web 22nd February 2005

2-Pyridone-fused 2,2'-bipyridine derivatives **1a** and **1b** were synthesised. X-Ray diffraction analysis of **1b** revealed a highly complex solid state structure with a disordered molecule imbedded in a channel structure formed by a centrosymmetric lattice of hexagonally packed, hydrogen bonded columns. The columns are assembled from three symmetry independent molecules. Dimerisation of the self-complementary *cis*-amide hydrogen bond motif is overridden by the fulfilment of the proton coordination ability of the phenanthroline nitrogens in accordance with Etter's rules of hydrogen bond priorities.

Introduction

Small and rigid, highly functionalised heterocyclic molecules are of interest as scaffolds for the construction of superstructures. Heterocycles provide hydrogen bonding and metal coordinating functionalities, offering strong and directional intermolecular interactions.¹ Appropriate positioning of those in a molecular skeleton will ideally lead to the formation of an aggregate of the desired structure.² For solution based aggregates, careful design is most often enough for success, given that entropy factors and solvent interactions are not neglected. In the solid state however, controlling or predicting the form of aggregation is much more difficult, since nucleation kinetics and packing requirements can severely perturb the thermodynamics of solution assembly. In addition, close packing brings the molecules in close contact, rendering weak intermolecular forces, not operating in solution, much more important in the solid state.³ Arrays of bi- and tridentate ligands have been synthesised and metal complexes thereof form helices, rosettes, grids and ladders *etc.* in solution and/or solid state.⁴ Numerous multicomponent assemblies of hydrogen bonding subunits have also been reported.⁵ Molecular aggregates based on both types of interactions include mainly solid state network structures.⁶

We are interested in the application of the self-complementary *cis*-amide hydrogen bonding motif for the assembly of functional aggregates from simpler components.⁷ We wanted to integrate this motif into a metal coordinating ligand, and investigate both the solution and solid state behaviour of the free ligand as well as its metal complexes. We chose the 2-pyridone moiety since it has been widely applied in the construction of molecular assemblies in solution⁸ and solid state, in purely organic structures⁹ as well as coordination complexes.¹⁰ 2,2'-Bipyridine was chosen as the ligand framework, being a rigid, bidentate ligand, so no competition should be expected from the *cis*-amide moiety in terms of coordination by a metal. Complexes with phenanthroline (phen) and terpyridine (tpy) based ligands with integrated hydrogen bonding functionalities have been utilised by other groups in constructing solid state networks.¹¹

We have thus fused the 2-pyridone and 2,2'-bipyridine moieties to obtain 9H-4,5,9-triazaphenanthren-10-one (**1**, Fig. 1), a

Janus molecule owing to its two different faces, one of hydrogen bonding, and one of metal coordination.¹² Upon complexation with metals, it should form solid state networks of alternating hydrogen bonding and metal coordination, the network dimensions being governed by the coordination properties of the metal.

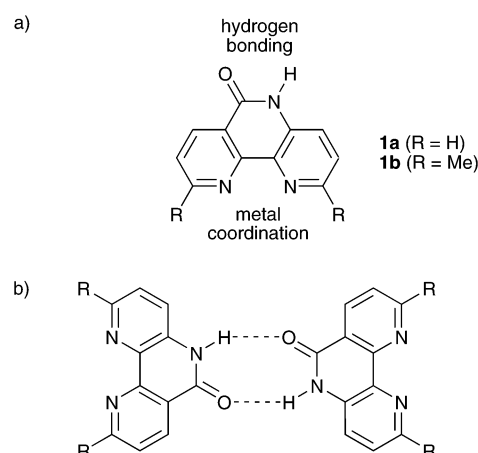
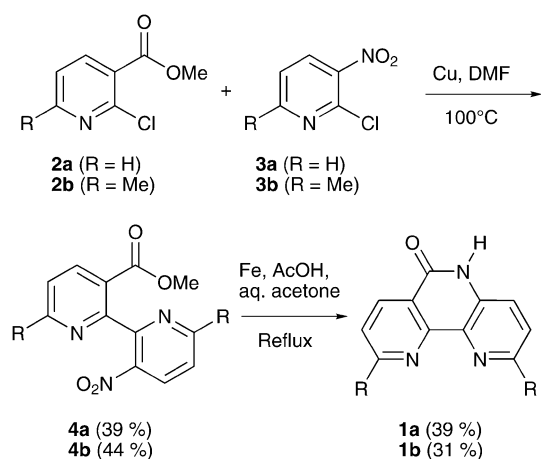


Fig. 1 (a) Janus molecules **1a** (R = H) and **1b** (R = Me). (b) The anticipated *cis*-amide back-to-back hydrogen bonding.

Looking at the structure of the free ligand **1** (Fig. 1a), one would anticipate it to aggregate to a back-to-back dimer due to the presence of the self-complementary 2-pyridone hydrogen bonding motif (Fig. 1b). However, to our surprise, the X-ray structural analysis of **1b** revealed a far more complicated structure. We now present the synthesis of ligands **1a** and **1b** as well as the surprisingly complex crystal structure of ligand **1b**, featuring self inclusion of a disordered guest molecule in a centrosymmetric host lattice, and the complete absence of the back-to-back dimer.

Results and discussion

Ligand **1a** was the original target molecule. It was synthesised in two steps, starting from chloropyridines **2a**¹³ and **3a** as shown in Scheme 1. Despite obvious yield limitations, the statistical



Scheme 1

Ullman coupling was chosen for the synthesis of 2,2'-bipyridine derivative **4a**, since initial efforts to prepare organometallic intermediates required for cross coupling were not fruitful. Thus, **4a** was obtained in 39% yield using copper powder in DMF. In the following reductive cyclisation, iron–acetic acid gave the best results out of the methods investigated, affording **1a** in 39% yield.

Ligand **1a** proved extremely insoluble in even the most polar aprotic solvents, making both purification and characterisation difficult. Furthermore, in all attempts to grow crystals, it crystallised as clusters of microscopic needles, and no single crystal of appropriate dimensions could be obtained.

Thus, in the hope for more amenable solubility and crystallisation properties, neocuproine analogue **1b** was synthesised following the same route as for **1a** (Scheme 1). Esterification of 6-methyl-2-chloronicotinic acid to produce **2b** resulted in low yields using a range of methods, including the one used to make **2a**. However, treatment with POCl₃ followed by MeOH afforded **2b** in an acceptable 69% yield. Chloropyridine **3b** was synthesised in two steps, by nitration of 2-amino-6-picoline,¹⁴ followed by diazotisation in hydrochloric acid.¹⁵ Finally, **1b** was obtained *via* Ullman coupling in 44% yield followed by reductive cyclisation in 31% yield, using the same procedures as for **1a**.

The two methyl substituents greatly improved the solubility, and rather large, thick, platelike single crystals were grown by slow diffusion of diethyl ether into a solution of **1b** in a 4 : 1 mixture of chloroform and methanol.

The crystal structure was solved in the triclinic, centrosymmetric space group *P* $\bar{1}$, with seven molecules in the unit cell (*Z*). The asymmetric unit contained three well resolved molecules (A, B and C, Fig. 2). After all the atoms in those three molecules had been located, the final difference Fourier map contained a number of peaks from which no reasonable molecular structure could be discerned. All the peaks were in the same plane,

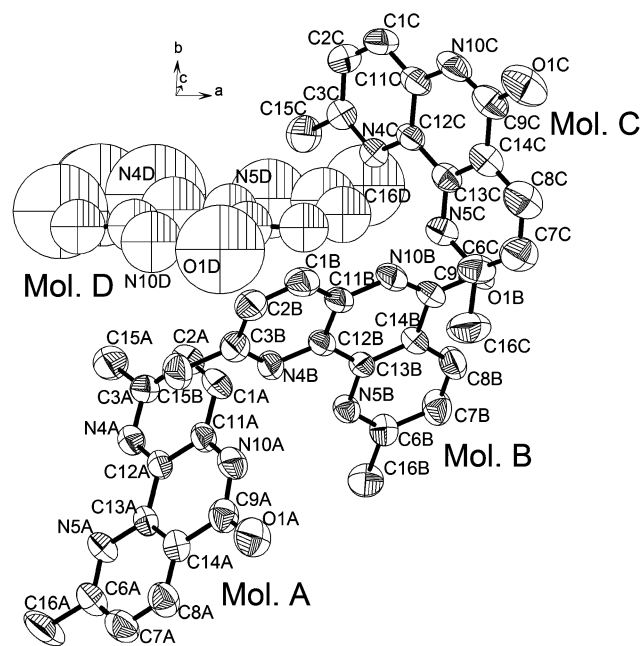


Fig. 2 DIAMOND drawing with atomic numbering of **1b**. Molecule D is shown in only one of its two possible orientations. It was refined isotropically and, as seen, the disorder gave rise to high isotropic displacement parameters. Hydrogens are omitted for clarity.

suggesting a polycyclic aromatic structure. Considering the lack of centrosymmetry in **1b** we concluded this to be a disordered, half molecule of **1b**. Attempts to resolve the disorder, either by solving the structure in the less symmetrical *P*1 space group or by low temperature data collection were unsuccessful.

The three well resolved molecules arrange into infinite columns propagating along the [111] axis, held together by four hydrogen bonds. Three of those are bifurcated, with the phen type nitrogen pairs acting as bidentate acceptors. The column structure is presented in Fig. 3 and the relevant hydrogen bond distances and angles are listed in Table 1. Molecule B serves as a bridge between π -stacked sandwiches of molecules A and C, respectively, fully utilising its hydrogen bonding capabilities.

The carbonyl oxygen of molecule A (O1A) forms weak, intercolumnar hydrogen bonds to aromatic C–H donors C2B and C2C. These hydrogen bonds provide direct contact points to four out of six neighbouring columns. As the columns pack together, channel structures are formed along the *a* axis (Fig. 4). Inside these channels, the disordered guest molecules line up in a plane parallel to the *a* axis. This was initially thought to be a clathrate. However, molecular modelling¹⁶ of **1b** inside the rigid channel with the disordered part of the crystal structure removed, revealed that random distribution of guest molecules along the channel is highly unlikely. Two symmetry-equivalent

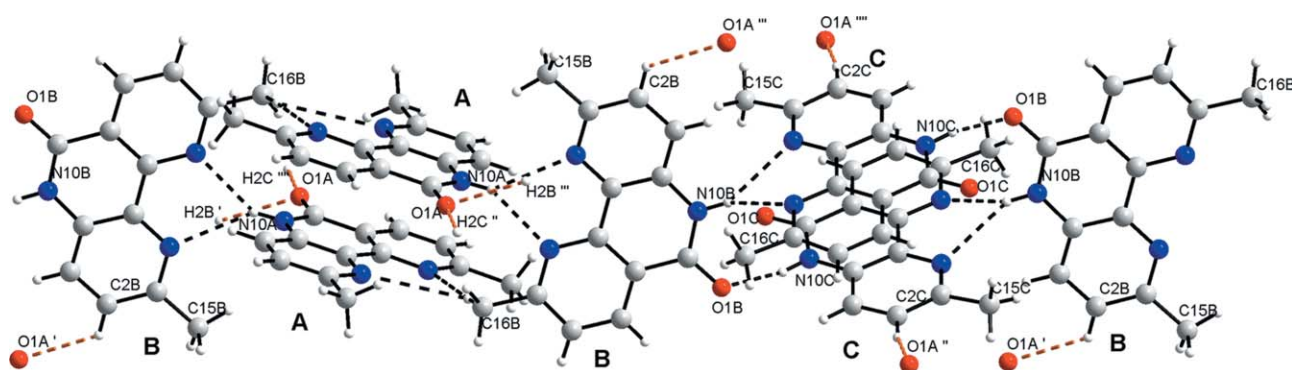


Fig. 3 Crystal structure of **1b**. Ball and stick model showing the arrangement of molecules A, B and C into a column structure along the [111] axis. Hydrogen bonds are shown as broken lines. Intercolumnar hydrogen bonds are orange. The prime symbols (') refer to different neighbouring columns.

Table 1 Hydrogen bond geometry in the infinite column structure

Donor atom ^a	Acceptor atom ^a	D...A/Å	D-H...A/°
N10A	N4B	3.200(35)	141.19(4)
N10A	N5B	3.057(33)	144.85(5)
C16B	N5A	3.551(64)	179.23(3)
C16B	N4A	3.548(43)	119.83(3)
N10B	N4C	3.298(38)	146.28(4)
N10B	N5C	3.011(21)	141.28(3)
N10C	O1B	2.845(11)	164.52(5)
C2C ^b	O1A	3.592(73)	155.13(3)
C2B ^b	O1A	3.383(19)	127.59(2)

^a For numbering see Fig. 2. ^b Intercolumnar hydrogen bonds.

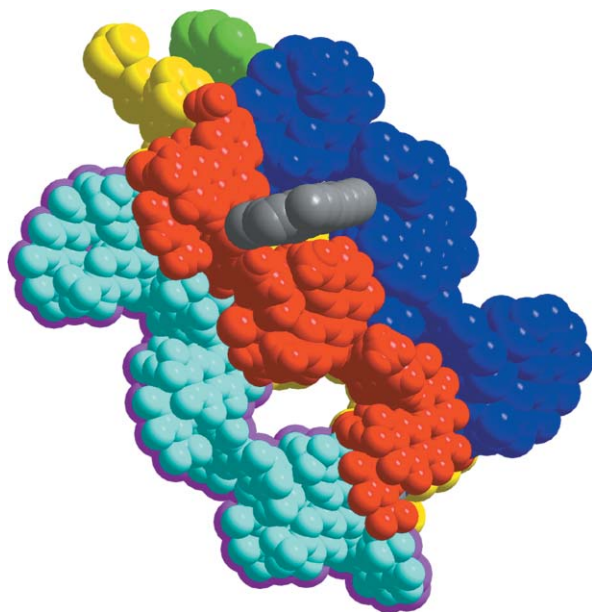


Fig. 4 Crystal structure of **1b**. A space filling model of a hexagonally packed array of seven columns viewed along the *a* axis. Each column has a representative colour. Two channels formed by the packing of the columns are shown, one is left empty for clarity and the other is filled with a guest molecule (grey).

orientations of **1b** (molecule D) are stabilised by interactions with the interior surface of the channel, making all other positions unfavourable. Overlaying **1b** in these orientations with the disordered part of the crystal structure reveals an almost perfect match. An inversion point in the centre of the disordered structure, at $(\frac{1}{2}, 1, 0)$ interrelates the two modelled orientations (Fig. 5a). It was thus concluded that the disordered structure represents two defined spatial orientations of **1b** at a specific position in the unit cell, each with an occupancy factor of 0.5. Two hydrogen bond acceptors (A), O1B and O1C, and one donor (D), C15C, line the interior surface of the channel. The potential interactions between these and the modelled guest structure are illustrated in Fig. 5b. To complete the structure refinement, the atomic coordinates of the modelled molecule D were applied to the crystal structure as a rigid group and the position of the rigid molecule was refined. The prediction of the molecular modelling was thereby confirmed in the crystal structure refinement. Interestingly, the occupancy factor for each of the two orientations of molecule D refined to 0.48, implying that 4% of the guest positions are empty (or perhaps filled with solvent). Some hydrogen bond interactions between molecule D and the surrounding lattice molecules are listed in Table 2.

Thus, despite the lack of symmetry in **1b**, molecule D complies with the centrosymmetry of the unit cell by adopting two centrosymmetrically related orientations. So the high number of molecules in the asymmetric unit ($Z' = 3.5$) does not fully describe the complexity of the crystal structure, since there are

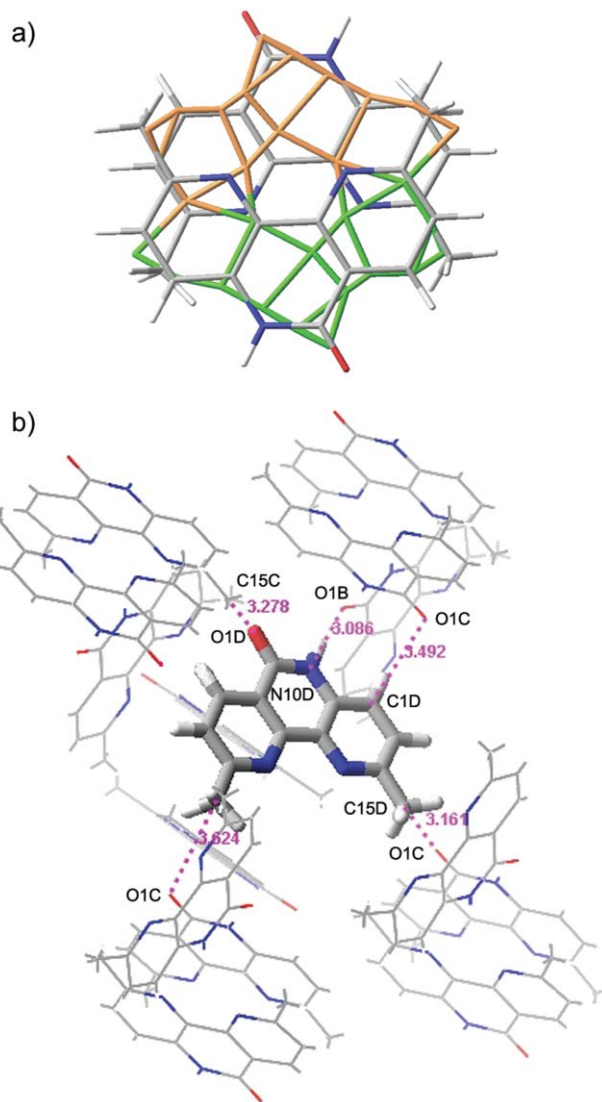


Fig. 5 Crystal structure of **1b**. Modelling of the guest in the rigid, empty channel structure. (a) Overlay of both possible orientations of molecule D according to molecular modelling (grey, C; red, O; blue, N) with the 15 carbons representing the disordered part of the crystal structure in the initial refinement (green and orange). The green atoms are created by centrosymmetry from the orange ones, while the two orientations of molecule D were modelled independently of each other. (b) The modelled guest inside the channel structure. The modelled structure is shown as a stick model while the crystal structure is a wire model. Possible hydrogen bonds are shown as pink dotted lines with the D...A distance.

Table 2 Some hydrogen bond distances between one of the two possible orientations of molecule D (guest) and the interior surface of the channel

Guest atom ^a	Atom in channel structure ^a	D...A/Å
C16D	O1C (<i>x</i> , <i>y</i> , $-1 + z$)	3.876
C15D	O1C ($-1 + x$, <i>y</i> , $-1 + z$)	3.460
C1D	O1C ($1 - x$, $2 - y$, $1 - z$)	3.544
N10D	O1B ($-1 + x$, <i>y</i> , <i>z</i>)	2.965
O1D	C15C (<i>x</i> , <i>y</i> , <i>z</i>)	3.558

^a For numbering see Fig. 2.

four possible halves of molecule D, all of which are equally represented by the disordered part of the crystal structure.

It appears that this unexpected crystal packing mode ($P\bar{1}$, $Z = 7$, $Z' = 3.5$) is quite an unusual one.¹⁷ A search in the Cambridge Structural Database (CSD)¹⁸ revealed that only two examples of this type of packing have been reported earlier.¹⁹ It is interesting to note that in both of these cases, like in the present one, the lack of centrosymmetry in the molecular structure is made up

for in the crystal packing by disordering one molecular unit out of four over two orientations at an inversion centre.

Bifurcated hydrogen bonds to the two phen nitrogens are prominent in the crystal structure of **1b**. This observation prompted a CSD¹⁸ search on the hydrogen bonding behaviour of phen derivatives in the solid state. Out of the 54 purely organic, nonionic 3D structures obtained, 36 included hydrogen bond interactions with the phen nitrogens.²⁰ 26 of these were solvates (H-bond donor being an OH or acidic CH of a solvent molecule from the crystallisation medium). While all of the 18 structures without hydrogen bonds to the phen nitrogens were devoid of donors in the molecular structure, this was true for only 17 of the solvate structures. This means that in only about 50 percent of the cases do donor free phen derivatives incorporate a donor containing solvent molecule into the crystal to fulfil their proton coordination ability, although this certainly relies on crystallisation conditions and medium. Further, of the 36 hydrogen bonded structures, 31 (86%) contained bifurcated hydrogen bonds to the phen nitrogen pair and 7 (19%) non-bifurcated ones. Two structures contained examples of both. This ratio was maintained in both solvate and non-solvate structures. Some recently published structures of phen-urea cocrystals²¹ support the notion that a high (>1) donor-acceptor ratio increases the probability of non-bifurcated hydrogen bonds to the phen nitrogens.

Due to an inappropriate bite angle, the two nitrogens rarely contribute equally to these bifurcated interactions, neither do they in our structure presented here. While the literature on hydrogen bonding behaviour of phen derivatives is scarce, one spectroscopic study²² shows that they form hydrogen bonds with phenols, that are 3–5 times stronger than expected from the correlation with pK_a in the pyridine series. Briefly, both the frequency shift in the phenol O–H stretching band in the IR spectrum, and the $-\Delta S$ term of the free energy of hydrogen bond formation, are smaller than for pyridines, suggesting either two low-energy positions for the proton in the field of the two nitrogen lone pairs, with rapid switching, or a broad, shallow energy minimum in the vicinity of the two acceptor atoms.²²

Given the self-complementarity of the *cis*-amide motif,²³ the crystal structure of **1b** was anticipated to consist of closely packed hydrogen bonded back-to-back dimers of the kind shown in Fig. 1b. Phenanthridone derivatives have been shown to form such dimers in solution²⁴ and phenanthridone itself crystallises as the dimer.²⁵ Still, given the rather large difference between the crystal structures of phenanthrene^{26a} and 1,10-phenanthroline,^{26b} resulting from the highly different charge distribution in the two compounds, one could argue that **1b** should not afford the same crystal structure as phenanthridone. Other compounds, structurally related to **1b**, such as neocuproine,^{26c} phenanthrene-9,10-dione^{26d} and 1,10-phenanthroline-5,6-dione^{26e} have quite simple and symmetric solid state structures.

So why does the expected back-to-back dimerisation yield to the unusual, apparently weaker (judging from the D...A distances in Table 1) bifurcated hydrogen bonds? Back-to-back dimerisation could be expected to result in higher symmetry and more efficient π -stacking but, without solvent incorporation, it would leave the nitrogen lone pairs of the bipyridine moiety uncompensated. According to Etter's rules,²⁷ the best acceptor in the crystallisation mixture, the phen nitrogen pair of **1b**, should hydrogen bond with the most acidic hydrogen. The amide hydrogen is considerably more acidic than the methanol crystallisation cosolvent OH (pK_a 17 (2-pyridone) vs. 28 (MeOH) in DMSO), and thus the best hydrogen bond donor. However, the self-complementarity and cooperativity of the 2-pyridone motif was expected to compensate for that, retaining the *cis*-amide dimer. Nevertheless, with a hydrogen bond donor-acceptor ratio of 1 : 3 in **1b**, the bifurcated interactions are an efficient way to compensate for the inherent donor deficiency. In one case, one of the relatively acidic methyl hydrogens of **1b** also serves as a weak

donor to a phen type nitrogen pair in an adjacent molecule of **1b**. The crystallisation process results from a very subtle balance of interactions. One favourable interaction can imply another unfavourable one. This fact is manifest in the presented crystal structure, where the strongest single interaction is sacrificed to allow the interaction potential of the whole structure to be satisfied.

In conclusion, we have presented the synthesis of 2-pyridone fused 2,2'-bipyridine derivatives, two faced (Janus) molecules with one potential hydrogen bonding face and one potential metal coordinating face. Our results highlight the 1,10-phenanthroline moiety as an efficient proton chelator, owing to its preorganised nitrogen pair. This property was the main driving force for the formation of an unexpectedly complex solid state structure of the free ligand **1b**, overriding the possible dimerisation of the self-complementary *cis*-amide hydrogen bond motif. Possible reasons for this could include the relatively high acidity of the 2-pyridone type NH proton which makes it a preferred hydrogen bond donor compared to solvent hydroxyl groups. Further, we have presented an example of an unusual crystal packing mode, containing three and a half molecules in the asymmetric unit and featuring self-inclusion in a channel type structure.

Experimental

General methods

2-Chloronicotinic acid methyl ester **2a**¹³ and 2-chloro-3-nitro-6-picoline **3b**^{14,15} were synthesised according to literature procedures. All other chemicals were used as received from commercial sources unless otherwise stated. TLC analyses (Merck 60 F₂₅₄ sheets) were visualised under UV light (254 nm). Column chromatography (CC) was performed with silica gel (Matrex 0.063–0.200 mm): column diameter 5 cm, length 12–18 cm and fraction sizes 30 mL. Melting points were determined in capillary tubes, using a Sanyo Gallenkamp melting point apparatus and are uncorrected. Infrared spectra were recorded on a Shimadzu FTIR-8300 spectrometer. NMR spectra were recorded on a Bruker DRX400 NMR spectrometer. Chemical shifts are given in ppm relative to TMS, using the residual solvent peaks at 7.27 (¹H) and 77.23 (¹³C) for CDCl₃ and 2.50 (¹H) and 39.51 (¹³C) for DMSO-d₆ as internal standards. Assignments were accomplished by coupling constants and integrals, as well as 2D correlation experiments when necessary.

Synthesis

2-Chloro-6-methylnicotinic acid methyl ester (2b). A suspension of 2-chloro-6-methylnicotinic acid (6.125 g, 35.7 mmol) in POCl₃ (25 mL) was heated at reflux for 2 h. A solution was attained upon heating. After distilling off the POCl₃ at reduced pressure, MeOH (72 mL) was added to the residue and the resulting solution was heated at reflux for 1.5 h. Evaporation of the solvent afforded a yellow solid. The pure product was obtained by bulb to bulb distillation at 85 °C and 0.3 mmHg, following a small fore fraction. Eluting the distillate through a silica pad with heptane–EtOAc (2 : 1) afforded pure **2b** (4.56 g, 24.6 mmol, 69%) as a colorless oil: mp 27–28 °C; R_f (heptane–EtOAc 2 : 1) 0.26; anal. calc. for C₈H₈ClNO₂: C, 51.77; H, 4.34; N, 7.55; found C, 51.73; H, 4.31; N, 7.59%; IR (KBr) cm⁻¹ 1735 (C=O, ester); δ_H (400 MHz, CDCl₃) 2.58 (3H, s), 3.93 (3H, s), 7.16 (1H, d, J = 7.9 Hz), 8.08 (1H, d, J = 7.9 Hz); δ_C (100 MHz, CDCl₃) 24.5, 52.9, 121.9, 123.7, 140.9, 149.6, 162.7, 165.2; HRMS (FAB+) m/z calc. for C₈H₈ClNO₂: 185.0244; found 185.0225.

3'-Nitro-2,2'-bipyridinyl-3-carboxylic acid methyl ester (4a). A mixture of **2a** (3.0 g, 17 mmol), **3a** (5.5 g, 35 mmol) and copper powder (6.0 g, 94 mmol) in distilled DMF (20 mL) was stirred at 100 °C. After 20 h, all starting materials were consumed

according to TLC. At room temperature, Na₂EDTA (32.0 g, 86 mmol) in water (300 mL) was added to the mixture. After stirring for 10 min, the copper was filtered off and washed with dichloromethane (5 × 30 mL). The filtrate was extracted with dichloromethane (5 × 30 mL). The combined organic phases were dried (Na₂SO₄) and the solvent was removed under reduced pressure to give 8.9 g of a brown oil containing some DMF. The crude product was chromatographed on a silica column using petroleum ether–EtOAc (1 : 2) as the eluent, affording **4a** (1.41 g, 5.44 mmol, 32%) as a pale orange solid: mp 82–84 °C; R_f (petroleum ether–EtOAc 1 : 2) 0.2; anal. calc. for C₁₂H₉N₃O₄: C, 55.60; H, 3.50; N, 16.21; found C, 55.54; H, 3.55; N, 16.04%; IR (KBr) cm⁻¹ 1724 (C=O, ester), 1527, 1348 (N=O); δ_H (400 MHz, CDCl₃) 3.72 (1H, s), 7.49 (1H, dd, *J* = 4.8, *J* = 8.0 Hz, 1H), 7.56 (1H, dd, *J* = 8.3, *J* = 4.7 Hz), 8.41 (1H, dd, *J* = 1.7, *J* = 8.0 Hz), 8.50 (1H, dd, *J* = 8.3, *J* = 1.5 Hz), 8.78 (1H, dd, *J* = 4.8, *J* = 1.7 Hz), 8.86 (1H, dd, *J* = 4.7, *J* = 1.5 Hz); δ_C (100 MHz, CDCl₃) 52.7, 123.6, 123.7, 125.2, 132.7, 138.8, 144.5, 152.4, 152.9, 154.0, 157.2, 165.6; HRMS (FAB+) *m/z* calc. for C₁₂H₉N₃O₄ [M + 1]⁺: 260.0666; found 260.0691.

6,6'-Dimethyl-3'-nitro[2,2']bipyridinyl-3-carboxylic acid methyl ester (4b). The product was synthesised from **2b** (0.87 g, 4.68 mmol) and **3b** (1.62 g, 9.38 mmol) according to the procedure for **4a**, except that the reaction time was 5 h and extraction was done with EtOAc. Purification by chromatography on a silica column using heptane–EtOAc (6 : 5) as the eluent provided **4b** (0.61 g, 2.12 mmol, 45%) as a light yellow solid: mp 126–127 °C; R_f (heptane–EtOAc 3 : 7) 0.3; anal. calc. for C₁₄H₁₃N₃O₄: C, 58.53; H, 4.56; N, 14.63; found C, 58.41; H, 4.48; N, 14.55%; IR (KBr) cm⁻¹ 1720 (C=O, ester), 1587, 1514, 1348 (N=O); δ_H (400 MHz, CDCl₃) 2.69 (3H, s), 3.71 (3H, s), 7.32 (1H, d, *J* = 8.1 Hz), 7.38 (1H, d, *J* = 8.5 Hz), 8.30 (1H, d, *J* = 8.1 Hz), 8.48 (1H, d, *J* = 8.5 Hz); δ_C (100 MHz, CDCl₃) 24.9, 25.0, 52.4, 122.0, 123.1, 123.2, 132.9, 139.0, 142.3, 153.8, 157.3, 162.5, 163.6, 165.6; HRMS (FAB+) *m/z* calc. for C₁₄H₁₄N₃O₄ [M + 1]⁺: 288.0979; found 288.0986.

9H-4,5,9-Triazaphenanthren-10-one (1a). A mixture of **4a** (1.51 g, 5.82 mmol), acetone (40 mL), glacial acetic acid (3.7 mL), water (3.7 mL) and powdered iron (1.35 g, 24.2 mmol) was refluxed for 3.5 h. The initial solution turned from yellow to dark yellow upon addition of iron, and when heated it turned intensely dark red, indicating complex formation. After cooling to room temperature, acetone was removed under reduced pressure. To the residue was added Na₂EDTA (8.1 g, 21.8 mmol) in water (80 mL), and NaOH (10 M, 7 mL). The mixture was stirred for 10 minutes. Unreacted iron was retained in the reaction flask using a magnet and the suspension was transferred and extracted with CH₂Cl₂ (6 × 150 mL) to obtain a yellow organic phase and a red aqueous phase with precipitate. The organic phases were separated and dried (Na₂SO₄). The solvent was removed under reduced pressure affording 80 mg of a brown powder, consisting of a mixture of products. Additional Na₂EDTA solution (12 g in 150 mL of water) was added to the aqueous phase. After stirring for 10 minutes, the red color turned yellow. A new extraction with CHCl₃–MeOH (9 : 1) (4 × 150 mL) provided pure **1a** (450 mg, 2.28 mmol, 39%) as a light yellow solid: mp 370 °C dec; R_f (MeOH–2 M NH₄Cl–MeNO₂ 7 : 2 : 1) 0.52 (displays a blue spot at 366 nm); anal. calc. for C₁₁H₇N₃O: C, 67.00; H, 3.58; N, 21.31; found C, 66.78; H, 3.67; N, 21.10%; IR (KBr) cm⁻¹ 1669, 1605, 1479, 1450, 1419; δ_H (400 MHz, DMSO-*d*₆) 7.61 (1H, dd, *J* = 8.3, *J* = 4.4 Hz), 7.77 (2H, m), 8.62 (1H, dd, *J* = 4.4, *J* = 1.5 Hz), 8.64 (1H, dd, *J* = 8.0, *J* = 1.8 Hz), 9.14 (1H, dd, *J* = 4.5, *J* = 1.8 Hz); δ_C (100 MHz, DMSO-*d*₆) 123.9, 124.2, 124.9, 126.1, 135.1, 136.1, 136.2, 145.1, 151.0, 155.0, 161.0; HRMS (FAB+) *m/z* calc. for C₁₁H₈N₃O [M + 1]⁺: 198.0662; found 198.0677.

3,6-Dimethyl-9H-4,5,9-triazaphenanthren-10-one (1b). The product was synthesised from **4b** (0.48 g, 1.67 mmol) according

to the procedure for **1a**, except that CH₂Cl₂ extraction (4 × 100 mL) of the aqueous phase afforded the crude product directly, as a red solid (0.26 g). Trituration with CH₂Cl₂ (2 × 10 mL) afforded **1b** (0.12 g, 0.53 mmol, 31%) as a white solid: mp 290 °C dec; R_f (CH₂Cl₂–MeOH 9 : 1) 0.33; anal. calc. for C₁₃H₁₁N₃O: C, 69.32; H, 4.92; N, 18.66; found C, 69.28; H, 5.08; N, 18.54%; IR (KBr) cm⁻¹ 1666, 1589, 1481, 1434, 1363; δ_H (400 MHz, DMSO-*d*₆) 2.59 (3H, s), 2.73 (3H, s), 7.44 (1H, d, *J* = 8.4 Hz), 7.48 (1H, d, *J* = 8.4 Hz), 7.59 (1H, d, *J* = 8.0 Hz), 7.64 (1H, d, *J* = 8.0 Hz), 11.81 (1H, br s); δ_C (100 MHz, DMSO-*d*₆) 23.9, 25.0, 121.1, 124.1, 124.2, 125.2, 132.6, 134.5, 135.8, 150.0, 152.6, 160.4, 163.7; HRMS (FAB+) *m/z* calc. for C₁₃H₁₂N₃O [M + 1]⁺: 226.0975; found 226.0974.

X-Ray crystallographic studies

Platelike single crystals were grown by slow diffusion of diethyl ether into a solution of **1b** in a 4 : 1 mixture of chloroform and methanol. Intensity data were collected at 293 K on a Bruker SMART CCD system using ω-scans and a rotating anode with Mo Kα radiation (λ = 0.71073 Å).²⁸ The intensity was corrected for Lorentz and polarisation effects using SADABS.²⁹ All reflections were integrated using SAINT.³⁰ The structure of **1b** was solved by direct methods and refined by full-matrix least-squares calculations on *F*² using SHELXTL 5.1.³¹ Non-disordered non-H atoms were refined with anisotropic displacement parameters. Aromatic hydrogen atoms were constrained to parent sites using a riding model, methyl hydrogens using a rotating model. From the difference Fourier map obtained after the three well-resolved molecules in the asymmetric unit had been located, a number of electron density peaks were obtained, all of them seemingly coplanar. Thus, the disordered molecule was represented by 15 isotropically refined carbon atoms in a plane, with an occupancy factor of 0.5, each of them having two symmetry-related positions. This refinement gave *wR*(*F*²) = 0.2666.

The optimal orientation of **1b** inside the channel according to molecular modelling (see below) was overlaid with the 15 carbon atoms corresponding to the strongest electron densities in the disordered part of the initial crystal structure refinement (see Fig. 5a). The agreement of these two structures was considered good enough to justify incorporation of the model structure into the crystal structure refinement. The 15 carbon atoms were thus removed and the atomic coordinates of the model structure were applied using a FRAG/FEND instruction. The position of the whole rigid molecule was refined and its overall occupancy factor of the two symmetry related positions was refined to 0.96. Non-hydrogen atoms were refined isotropically and hydrogen atoms were not included.

Crystal data. C₁₁H₁₃N₃O. *M* = 225.25, triclinic, *P* $\bar{1}$, *a* = 10.0572, *b* = 13.7223, *c* = 15.4233 Å, *a* = 72.173, β = 80.393, γ = 86.903°, *V* = 1997.7 Å³, *D*_{calcd} = 1.301 g cm⁻³, *Z* = 7, μ = 0.086 mm⁻¹. 21513 reflections measured, 11415 unique (*R*_{int} = 0.0440) which were used in all calculations. The final *wR*(*F*²) was 0.3289 and the *S* value 1.161 (all data). The *R*(*F*) was 0.0977 (*I* > 2σ(*I*)).†

Molecular modelling

In the program Diamond V2.0e, the crystal structure of **1b** was extended along the crystallographic *a* axis using symmetry operations. The disordered part of the structure was removed to create a hollow channel defined by 33 molecules of **1b**, spanning approx. 25 Å along the *a* axis. The atomic coordinates were transferred to the program Macromodel¹⁶ where the correct atom types and bond orders were defined. Keeping all 33 molecules from the crystal structure fixed at their coordinates,

† CCDC reference numbers 256289. See <http://www.rsc.org/suppdata/ob/b4/b417485b/> for crystallographic data in .cif or other electronic format.

the inside of the channel structure was probed by one molecule of **1b** by energy minimising it from variable starting orientations and positions inside the channel, using the MMFF force field.³²

CSD search

The search was conducted using CSD version 5.25 (November 2003).¹⁸ A query consisting of the parent phenanthroline structure resulted in 86 crystal structures of purely organic, nonionic composition. Entries containing N-substitution or chelation by alkali metals (24) were eliminated by hand, as well as those missing a 3D structure (8), leaving 54 structures to be analysed.

Acknowledgements

We thank the Swedish Research Council as well as the Crafoord Foundation, the Lars-Johan Hjerta Foundation, the Magn. Bergvall Foundation and the Royal Physiographic Society for generous grants. The faculty exchange program between Lund University and the University of California is acknowledged for a scholarship to K. W.

References

- 1 S. C. Zimmerman and P. S. Corbin, *Struct. Bonding (Berlin)*, 2000, **96**, 63; J. A. R. Navarro and B. Lippert, *Coord. Chem. Rev.*, 1999, **185–186**, 653.
- 2 J.-M. Lehn, *Supramolecular Chemistry-Concepts and Perspectives*, Wiley-VCH, Weinheim, 1995.
- 3 A. Gavezotti, *Faraday Discuss.*, 1997, **106**, 63; A. Gavezotti, *Acc. Chem. Res.*, 1994, **27**, 309.
- 4 G. F. Swiegers and T. J. Malefetse, *Chem. Rev.*, 2000, **100**, 3483 and references therein.
- 5 L. J. Prins, D. N. Reinhoudt and P. Timmerman, *Angew. Chem., Int. Ed.*, 2001, **40**, 2382 and references therein.
- 6 A. M. Beatty, *CrystEngComm*, 2001, **3**, 243 and references therein.
- 7 S. Jönsson, F. G. J. Odille, P.-O. Norrby and K. Wärnmark, *Chem. Commun.*, 2005, 549; S. Stončius, E. Butkus, A. Zilinskas, K. Larsson, L. Öhrström, U. Berg and K. Wärnmark, *J. Org. Chem.*, 2004, **69**, 5196.
- 8 S. C. Zimmerman and B. F. Duerr, *J. Org. Chem.*, 1992, **57**, 2215; M. Gallant, M. T. P. Viet and J. D. Wuest, *J. Org. Chem.*, 1991, **56**, 2284; Y. Ducharme and J. D. Wuest, *J. Org. Chem.*, 1988, **53**, 5789.
- 9 T. Olszewska, M. Gdaniec and T. Polonski, *J. Org. Chem.*, 2004, **69**, 1248; Y. Du, C. J. Creighton, B. A. Tounge and A. B. Reitz, *Org. Lett.*, 2004, **6**, 309; M. R. Edwards, W. Jones and W. D. S. Motherwell, *Cryst. Eng.*, 2002, **5**, 25; C. B. Aakeröy, A. M. Beatty, M. Nieuwenhuyzen and M. Zou, *Tetrahedron*, 2000, **56**, 6693; E. Murguly, R. McDonald and N. R. Branda, *Org. Lett.*, 2000, **2**, 3169; M. Akazome, S. Suzuki, Y. Shimizu, K. Henmi and K. Ogura, *J. Org. Chem.*, 2000, **65**, 6917; M. Simard, D. Su and J. D. Wuest, *J. Am. Chem. Soc.*, 1991, **113**, 4696.
- 10 M. Munakata, L. P. Wu, M. Yamamoto, T. Kuroda-Sowa and M. Maekawa, *J. Am. Chem. Soc.*, 1996, **118**, 3117; S. R. Breeze and S. Wang, *Inorg. Chem.*, 1993, **32**, 5981.
- 11 D. G. Kurth, K. M. Fromm and J.-M. Lehn, *Eur. J. Inorg. Chem.*, 2001, 1523; U. Ziener, E. Breuning, J.-M. Lehn, E. Wegelius, K. Rissanen, G. Baum, D. Fenske and G. Vaughan, *Chem.-Eur. J.*, 2000, **6**, 4132.
- 12 Janus was the Roman god of change and transition. He had two faces looking in opposite directions, hence the analogy with **1**.
- 13 F. Leroy, P. Després, M. Bigan and D. Blondeau, *Synth. Commun.*, 1996, **26**, 2257.
- 14 J. Ohmori and H. Kubota, *J. Med. Chem.*, 1996, **39**, 1331.
- 15 R. Troschütz and A. Karger, *J. Heterocycl. Chem.*, 1996, **33**, 1815.
- 16 Macromodel V6.0. F. Mohamadi, N. G. J. Richards, W. C. Guide, R. Liskamp, M. Lipton, C. Caulfield, G. Chang, T. Hendrickson and W. C. Still, *J. Comput. Chem.*, 1990, **11**, 440.
- 17 For a discussion on Z' and crystal packing frequencies see: T. Steiner, *Acta Crystallogr., Sect. B*, 2000, **56**, 673; C. P. Brock, *Chem. Mater.*, 1994, **6**, 1118.
- 18 *CCDC, Cambridge Structural Database CSD 1.6*. University of Cambridge, UK, 2003.
- 19 T. Steiner, J. van der Maas and B. Lutz, *J. Chem. Soc., Perkin Trans. 2*, 1997, 1287; L. Kaczmarek, R. Balicki, J. Lipkowski and P. Borowicz, *J. Chem. Soc., Perkin Trans. 2*, 1994, 1603.
- 20 For selected hydrogen bonded structures see: D. Paul, F. Melin, C. Hirtz, J. Wytko, P. Ochsenbein, M. Bonin, K. Schenk, P. Maltese and J. Weiss, *Inorg. Chem.*, 2003, **42**, 3779; E. S. Lavender, R. M. Gregson, G. Ferguson and C. Glidewell, *Acta Crystallogr., Sect. C*, 1999, **55**, 751; E. García-Martínez, E. M. Vázquez-López and D. G. Tuck, *Acta Crystallogr., Sect. C*, 1998, **54**, 840; Y.-P. Tian, C.-Y. Duan, X.-X. Xu and X.-Z. You, *Acta Crystallogr., Sect. C*, 1995, **51**, 2309; W. H. Watson, J. Galloy, F. Vögtle and W. M. Müller, *Acta Crystallogr., Sect. C*, 1984, **40**, 200.
- 21 P. S. Donnelly, B. W. Skelton and A. H. White, *Aust. J. Chem.*, 2003, **56**, 1249.
- 22 G. G. Siegel and Th. Zeegers-Huyskens, *Spectrochim. Acta, Part A*, 1989, **45A**, 1297.
- 23 The literature does contain examples where the *cis*-amide motif fails to form the hydrogen bonded dimer in the solid state, see: E. F. Maverick, P. L. Wash and D. A. Lightner, *Acta Crystallogr., Sect. C*, 2001, **57**, 284; É. Boucher, M. Simard and J. D. Wuest, *J. Org. Chem.*, 1995, **60**, 1408; M.-J. Brienne, J. Gabard, M. Leclercq, J.-M. Lehn, M. Cesario, C. Pascard, M. Chevè and G. Dutruc-Rosset, *Tetrahedron Lett.*, 1994, **35**, 8157.
- 24 R. Kleppinger, C. P. Lillya and C. Yang, *J. Am. Chem. Soc.*, 1997, **119**, 4097.
- 25 D. K. Sen, *Acta Crystallogr., Sect. B*, 1970, **26**, 1629.
- 26 (a) V. Petříček, I. Čiřáková, L. Hummel, J. Kroupa and B. Březina, *Acta Crystallogr., Sect. B*, 1990, **46**, 830; (b) S. Nishigaki, H. Yoshioka and K. Nakatsu, *Acta Crystallogr., Sect. B*, 1978, **34**, 875; (c) D. K. Sen, *Acta Crystallogr., Sect. B*, 1969, **25**, 988; (d) M. Alleaume, R. Darrouy and J. Housty, *Acta Crystallogr.*, 1961, **14**, 1202; (e) F. Calderazzo, F. Marchetti, G. Pampaloni and V. Passarelli, *J. Chem. Soc., Dalton Trans.*, 1999, 4389.
- 27 M. C. Etter, *Acc. Chem. Res.*, 1990, **23**, 120.
- 28 BrukerAXS, SMART, Area Detector Control Software, Bruker Analytical X-ray System, Madison, Wisconsin, USA, 1995.
- 29 G. M. Sheldrick, *SADABS, Program for Absorption Correction*, University of Göttingen, Germany, 1996.
- 30 BrukerASX, SAINT, Integration Software, Bruker Analytical X-ray System, Madison, Wisconsin, USA, 1995.
- 31 G. M. Sheldrick, *SHELXTL 5.1, Program for Structure Solution and Least Square Refinement*, University of Göttingen, Germany, 1998.
- 32 T. A. Halgren, *J. Comput. Chem.*, 1996, **17**, 490.